AMERICAN SOCIETY FOR MICROBIOLOGY | Applied and Environmental Microbiology

Dissection of *Francisella*-Host Cell Interactions in *Dictyostelium discoideum*

Elisabeth O. Lampe,[a,b] Yannick Brenz,[c] Lydia Herrmann,[c] Urska Repnik,[d] Gareth Griffiths,[d] Carl Zingmark,[e] Anders Sjöstedt,[f] Hanne C. Winther-Larsen,[a,b] Monica Hagedorn[c]

Centre for Integrative Microbial Evolution (CIME)[a] and Department of Pharmaceutical Biosciences, School of Pharmacy, University of Oslo, Oslo, Norway[b]; Section of Parasitology, Bernhard Nocht Institute for Tropical Medicine, Hamburg, Germany[c]; Department of Biosciences, University of Oslo, Oslo, Norway[d]; Department of Molecular Biology, Umeå Centre for Microbial Research, Umeå University, Umeå, Sweden[e]; Department of Clinical Microbiology, Clinical Bacteriology, and Laboratory for Molecular Infection Medicine Sweden (MIMS), Umeå University, Umeå, Sweden[f]

Francisella **bacteria cause severe disease in both vertebrates and invertebrates and include one of the most infectious human pathogens. Mammalian cell lines have mainly been used to study the mechanisms by which *Francisella* manipulates its host to replicate within a large variety of hosts and cell types, including macrophages. Here, we describe the establishment of a genetically and biochemically tractable infection model: the amoeba *Dictyostelium discoideum* combined with the fish pathogen *Francisella noatunensis* subsp. *noatunensis*. Phagocytosed *F. noatunensis* subsp. *noatunensis* interacts with the endosomal pathway and escapes further phagosomal maturation by translocating into the host cell cytosol. *F. noatunensis* subsp. *noatunensis* lacking IglC, a known virulence determinant required for *Francisella* intracellular replication, follows the normal phagosomal maturation and does not grow in *Dictyostelium*. The attenuation of the *F. noatunensis* subsp. *noatunensis* Δ*iglC* mutant was confirmed in a zebrafish embryo model, where growth of *F. noatunensis* subsp. *noatunensis* Δ*iglC* was restricted. In *Dictyostelium*, *F. noatunensis* subsp. *noatunensis* interacts with the autophagic machinery. The intracellular bacteria colocalize with autophagic markers, and when autophagy is impaired (*Dictyostelium* Δ*atg1*), *F. noatunensis* subsp. *noatunensis* accumulates within *Dictyostelium* cells. Altogether, the *Dictyostelium-F. noatunensis* subsp. *noatunensis* infection model recapitulates the course of infection described in other host systems. The genetic and biochemical tractability of the system allows new approaches to elucidate the dynamic interactions between pathogenic *Francisella* and its host organism.**

The genus *Francisella* comprises Gram-negative, facultative intracellular bacteria that infect a wide range of species, including protozoa, invertebrates, and vertebrates (1–3). *Francisella* species can be divided into two lineages represented by *Francisella tularensis*, causing potentially fatal tularemia in humans, and *Francisella noatunensis*, infecting aquatic animals (4–6). The high infectivity (<10 CFU lethal dose) of *F. tularensis* (7) and its potential use for biological warfare (8) has generated increasing interest during the last decade in dissecting the interactions between pathogenic *Francisella* and its host at both the cellular and organism levels.

F. noatunensis shares high infectivity and a common core set of genes with the human pathogen *F. tularensis* (6). *F. noatunensis* is divided into two subspecies, *F. noatunensis* subsp. *noatunensis* and *F. noatunensis* subsp. *orientalis*, causing major problems in aquaculture based on Atlantic cod and tilapia, respectively (9). *F. noatunensis* subsp. *orientalis* generally causes a more aggressive disease, with up to 95% mortality (10). In Atlantic cod, its natural host, *F. noatunensis* subsp. *noatunensis* commonly causes a chronic systemic disease with tularemia-like symptoms, including granulomas in skin and internal organs (11). Preliminary studies in Atlantic cod cells suggest that the infection of phagocytic cells recapitulates the infection of mammalian macrophages with *F. tularensis* (12).

Francisella is able to invade and replicate in both phagocytic and nonphagocytic cell types, with macrophages being the predominant target cells (8, 13). After cell entry, the *Francisella*-containing phagosome interacts with the endosomal pathway and is transiently acidified (14–16). Subsequently, the bacteria escape the phagosome into the cytosol, thereby avoiding phagolysosomal fusion and degradation (14, 15, 17, 18). Within the cytosol, *Francisella* replicates extensively, a process that leads to the death of human and murine macrophages *in vitro* and the release of bacteria, which can reinfect new host cells (19, 20). Inside the macrophage cytosol, *Francisella* has been shown to be targeted for autophagic degradation by ubiquitination and recruitment of p62 (21); however, the role of autophagy in *Francisella* infections is still disputed and varies between host cell models. In human macrophages, *F. tularensis* avoids autophagic degradation (21–23) but is able to exploit the autophagic process by harvesting amino acids from degraded material (24). In murine macrophages, bacteria can reenter autophagic vacuoles after cytosolic replication, which has been suggested to help bacterial egress (25).

The virulence mechanisms of *Francisella* are still poorly understood despite thorough examination in many different hosts (26). The most prominent set of virulence genes is encoded within the 30-kb *Francisella* pathogenicity island (FPI) (27, 28). While *F.*

Received 21 September 2015 **Accepted** 22 December 2015

Accepted manuscript posted online 28 December 2015

Citation Lampe EO, Brenz Y, Herrmann L, Repnik U, Griffiths G, Zingmark C, Sjöstedt A, Winther-Larsen HC, Hagedorn M. 2016. Dissection of *Francisella*-host cell interactions in *Dictyostelium discoideum*. Appl Environ Microbiol 82:1586–1598. doi:10.1128/AEM.02950-15.

Editor: E. G. Dudley, Pennsylvania State University

Address correspondence to Monica Hagedorn, hagedorn@bnitm.de.

Y.B. and E.O.L. contributed equally to this work.

Supplemental material for this article may be found at http://dx.doi.org/10.1128/AEM.02950-15.

tularensis subsp. *tularensis* and *F. tularensis* subsp. *holarctica* have two FPI copies in their genomes, *Francisella novicida*, *Francisella philomiragia*, and *F. noatunensis* subsp. *orientalis* have only one FPI (29, 30). The incomplete assembly of the *F. noatunensis* subsp. *noatunensis* genome suggests that the *F. noatunensis* subsp. *noatunensis* genome contains a single FPI (GOLD analysis [92] project identifier [ID], Ga0010024). Knockout mutants of most FPI genes display attenuated intracellular growth, often accompanied by an inability to escape the phagosome (31–34). Notably, deletion of intracellular growth locus C (*iglC*) blocks escape from the phagosome and causes failure to induce apoptosis and downregulation of host signaling (20, 35, 36). IglC is suggested to form the inner tube of a type 6 secretion system but is also secreted into the host cell cytosol (37). Expression of *iglC* is highly upregulated during intracellular growth (38), and intriguingly, IglC is the most abundant protein identified in outer-membrane vesicles (OMVs) secreted by *F. noatunensis* subsp. *noatunensis* (39).

Several infection models are available to study *Francisella* infection *in vivo* (40) and *in vitro* (18, 41). Among animal models, mice are predominantly used, due to the wide spectrum of available genetic tools, but their susceptibilities to different *F. tularensis* strains differ drastically from those of humans (7, 40, 42). Research on intracellular aspects of *Francisella* infection is predominantly performed *in vitro* using human and murine macrophages. However, these host cell models show major differences in their responses to *Francisella* infection, such as inflammatory cytokine production (41, 43), as well as different interactions with the autophagic pathway (21, 25). Therefore, the development of alternative infection systems to study *Francisella* gained special interest, as indicated by the rising number of models, i.e., *Drosophila melanogaster* (*in vivo* and *in vitro*) (44, 45), zebrafish (46, 47), and amoeba (1, 3). These models may not present all features of the natural host infection, but they complement the currently used systems on the organism and cellular levels. They also have the power to reveal conserved bacterial and host strategies independent of specific model systems.

Amoebae are suggested to be the natural reservoir for waterborne tularemia, supported by the ability of *F. tularensis* and *F. novicida* to survive and replicate within the amoebae *Acanthamoeba castellanii* (1, 3, 48) and *Hartmannella vermiformis* (3), respectively. It has been suggested that bacterial virulence in amoebae and macrophages is mediated by similar mechanisms. For example, IglC is essential for *Francisella* survival and growth in both systems (49). A similar principle is conserved in *Legionella* infections (50).

In this study, we established a *Francisella* infection model using the amoeba *Dictyostelium discoideum* as a surrogate macrophage and *F. noatunensis* subsp. *noatunensis*, which has an optimal growth temperature similar to that of the *Dictyostelium* host, as a pathogen. Basic processes of host-pathogen interactions, such as phagocytosis, phagosomal maturation, and autophagy, are evolutionarily well conserved and very similar between *Dictyostelium* and macrophages (51–53). The easy and cheap handling in the laboratory, as well as the vast availability of *Dictyostelium* mutant strains, makes the amoeba a useful tool to dissect host-pathogen interactions. *Dictyostelium* is successfully established as a model to dissect host-pathogen interactions using a wide range of pathogenic bacteria, such as *Legionella*, *Mycobacterium*, and *Pseudomonas* (54–56). Our study shows that infection of *Dictyostelium* with *F. noatunensis* recapitulates the cellular aspects of *Francisella* infection of mammalian macrophages and presents a useful model to map the interactions between pathogenic *Francisella* bacteria and their phagocytic host cells.

MATERIALS AND METHODS

Host cells, bacterial strains, and culture conditions. Wild-type (wt) *Dictyostelium* cells (Ax2) were cultured axenically as described previously (55). *Dictyostelium* Δ*atg1* cells have been described (57). *F. noatunensis* subsp. *noatunensis* isolated from diseased Atlantic cod (*Gadus morhua L.*) in Norway were transformed with a green (pKK289km::*gfp*) (58) or red (pKK289km::*mCherry*) fluorescent plasmid and were grown as described previously (46) unless otherwise stated.

Comparison of the *igl* locus of *F. noatunensis* subsp. *noatunensis* FSC769 with those of other *Francisella* species. The *F. noatunensis* subsp. *noatunensis* FSC769 sequencing data were accessed as contigs from the GOLD analysis project (ID, Ga0010024), among which contig 16 contains the *igl* locus. Sequence comparison was performed in CLC Workbench 6.6.2 (CLC bio, Aarhus, Denmark). The sequences selected for comparison were *F. noatunensis* subsp. *orientalis* LADL-07-285A (GI 564747871), *F. philomiragia* ATCC 25017 (GI 167596226), *F. novicida* U112 (GI 754269614), *F. tularensis* subsp. *holarctica* LVS (GI 754265763), and *F. tularensis* subsp. *tularensis* Schu S4 (GI 754282044).

Construction of the *F. noatunensis* subsp. *noatunensis* Δ*iglC* mutant and the *F. noatunensis* subsp. *noatunensis iglC*$^+$ complementation strain. The method used to construct the *F. noatunensis* subsp. *noatunensis* Δ*iglC* knockout construct was derived from Golovliov et al. (18) and is similar to the knockout construction done by Lindgren et al. (59). The primers are listed in Table S1 in the supplemental material. In short, the two ~1,100-bp flanking regions of *iglC* were amplified using primers P1 to P4, and the PCR products were fused together through splicing by overhang extension (SOE) PCR (see Table S1 in the supplemental material, P1 and P4). The resulting knockout construct was ligated into the pGEM-T Easy vector (Promega, Madison, WI, USA) and further subcloned into the pDMK2 vector (60) using the restriction enzymes Fast Digest NotI and Fast Digest MluI (Life Technologies, Carlsbad, CA, USA). The final pDMK2::Δ*iglC* construct was transformed into electrocompetent *Escherichia coli* S17-1 (61).

E. coli S17 pDMK2::Δ*iglC* was grown to an optical density at 600 nm (OD_{600}) of 0.4 to 0.5. *F. noatunensis* subsp. *noatunensis* was cultured for 2 days at 20°C and 100 rpm, and the OD_{600} was adjusted to 1. Both *F. noatunensis* subsp. *noatunensis* and *E. coli* were pelleted and resuspended in phosphate-buffered saline (PBS), and conjugation suspensions of *F. noatunensis* subsp. *noatunensis* and *E. coli* were deposited as 50-μl drops onto ECFA plates (62) and incubated at 20°C overnight. The colony material was washed once in PBS before being resuspended in PBS, spread on ECFA plates containing 10 μg/ml kanamycin and 75 μg/ml polymyxin, and incubated at 20°C. Colonies appeared after 2 weeks and were screened with primer sets P2 plus P5 and P1 plus P6. The resulting strain, *F. noatunensis* subsp. *noatunensis* pDMK2::Δ*iglC*, was suspended in PBS, and 10-fold dilutions were plated onto ECFA containing 5% sucrose and incubated at 20°C. Colonies appeared after 2 weeks and were screened with primer set P5 plus P7 and *F. noatunensis* subsp. *noatunensis groEL* primers P8 and P9. Sequencing verified an in-frame deletion, and quantitative PCR (qPCR) with primers Q13 to Q16 confirmed no polar effects on the flanking genes, *iglB* and *iglD*.

The *iglC* gene was amplified with an Expand Long Range polymerase kit (Roche, Basel, Switzerland) and primers P10 and P11 using genomic DNA (gDNA) from *F. noatunensis* subsp. *noatunensis* wt as the template. *iglC* was ligated into pKK289Km (63) after digestion of the PCR product and the expression plasmid pKK289Km::*gfp* with the restriction enzymes NdeI and EcoRI (New England BioLabs Inc., Ipswich, MA, USA). The insert sequence was verified by Sanger sequencing using an Applied Biosystems sequencer at the University of Oslo. Transformation of pKK289Km::*iglC* into *F. noatunensis* subsp. *noatunensis* Δ*iglC* was per-

formed essentially as described by Bakkemo et al. (12), and the product was designated *F. noatunensis* subsp. *noatunensis* Δ*iglC*$^{+}$.

Plaque assay. Five hundred microliters of *Klebsiella* and 1,000 ml of *F. noatunensis* subsp. *noatunensis* and *F. noatunensis* subsp. *noatunensis* Δ*iglC* cultures were centrifuged for 15 min at 5,000 × *g* and 10,000 × *g*, respectively. The pellets were washed twice with Sørensen buffer (2 g/liter KH_2PO_4, 0.29 g/liter Na_2HPO_4; pH 6), and the resuspended bacteria were mixed with 50 *Dictyostelium* cells in Sørensen buffer. The *Dictyostelium*-bacteria suspensions were spread on separate starvation plates (Sørensen buffer plus agar) and dried. The plates were incubated at 21°C and observed regularly for plaque formation on the following days.

Infection assay. *F. noatunensis* subsp. *noatunensis* was grown until it reached the exponential growth phase (64). Bacteria (multiplicity of infection [MOI] = 30) were washed and resuspended in HL5-C (For-Medium, Hunstanton, United Kingdom) for infection. *Dictyostelium* cells were grown without antibiotics to a confluence of 80 to 100%. On the day of infection, bacteria were centrifuged onto the cell monolayer at 100 × *g* and 21°C for 30 min using swing-out rotors and subsequently left to phagocytose for 5 min. Free bacteria were washed off with HL5-C. Finally, the infected cells were seeded in 10-cm tissue culture dishes at various time points and cell numbers (2, 4, and 6 h postinfection [hpi], 1×10^7; 24 hpi, 4.5×10^6; 48 hpi, 2×10^6). At each time point, the cells were resuspended, counted, and either fixed to examine the infection by microscopy and flow cytometry or frozen at −20°C to measure genome equivalents by qPCR. For flow cytometry, 1×10^6 cells were centrifuged (500 × *g*; 2 min; room temperature) in fluorescence-activated cell sorter (FACS) tubes and fixed with 4% paraformaldehyde (PFA) in Sørensen buffer for 1 h at room temperature or at 4°C overnight. Fixation was stopped with 100 mM glycine-PBS for 5 min. For manual counting of the bacterial load by wide-field fluorescence microscopy (Carl Zeiss AG, Oberkochen, Germany, and Olympus Europa Holding GmbH, Hamburg, Germany), a minimum of 100 *Dictyostelium* cells were scored and categorized. For flow cytometry analysis, the green fluorescence representing bacteria was expressed as the number of relative fluorescence units (RFU) per unit volume (milliliter) of cell culture. Therefore, the infection rate was multiplied by the *Dictyostelium* cell growth (cells per milliliter) to obtain the number of infected cells per milliliter. This value was multiplied by the mean green-fluorescence (FL-1) value of *Francisella* bacteria only, which was calculated as the mean FL-1 of infected cells minus the mean FL-1 of noninfected cells. All samples were analyzed at the same fluorescence detector settings. At least 40,000 cells were analyzed per sample using a FACSCalibur flow cytometer (Becton Dickinson, Franklin Lakes, NJ, USA). Calculations were done in Excel and GraphPad Prism (GraphPad Software Inc., La Jolla, CA, USA).

In association studies of fixed samples, positive associations with p80 and VatA were verified when bacteria were fully enclosed within a p80- or VatA-positive vacuole. Positive ubiquitin association was counted when the bacteria were coated with longitudinal patches or full rings of ubiquitin. Adjacency of ubiquitin dots was not considered.

Antibodies. Mouse primary antibodies against the following antigens were obtained: p80 (65) from P. Cosson (University of Geneva, Geneva, Switzerland), VatA (66) from M. Maniak (Kassel University, Kassel, Germany), and FK2H (anti-polyubiquitinylated conjugates) from Enzo (Farmingdale, NY, USA). Rabbit polyclonal antibody against green fluorescent protein (GFP) was bought from MBL International (Woburn, MA, USA). Secondary antibodies were goat anti-rabbit or anti-mouse coupled to Alexa Fluor 488 and 558, respectively (Invitrogen, Carlsbad, CA, USA).

Immunolabeling. Immunolabeling for microscopy was performed on coverslips as described previously (67). Primary antibodies were used as followed: p80/VatA, 1:10; ubiquitin, 1:1,000, and GFP, 1:1,000. Secondary antibodies were used at 1:1,000.

For flow cytometry analysis, PFA-fixed cells were blocked (0.5% fetal calf serum [FCS], 0.1% Triton in PBS for 20 min), centrifuged (500 × *g*; 5 min; room temperature), and incubated in primary antibody solution (α-GFP; 1:1,000 in blocking solution) for 1 h. After two washes with blocking solution, the cells were stained for 1 h with secondary antibody solution (goat α-rabbit 488), washed twice, and resuspended in PBS for flow cytometry analysis.

Live imaging. For live imaging, infected cells were placed in a 35-mm μ-dish (Ibidi, Martinsried, Germany) at the appropriate times of infection in filtered HL5-C medium. Imaging was performed with either an Olympus IX81 wide-field fluorescence microscope (Olympus Europa Holding GmbH, Hamburg, Germany) equipped with a 60× UPlanSApo oil immersion objective (numerical aperture [NA] 1.35) at 21°C with 10-s intervals or a Zeiss LSM 5 live confocal microscope (Carl Zeiss AG, Oberkochen, Germany) with a 100× Europlan Apochromat oil immersion objective (NA 1.4), a diode laser 488, and a DPSS (diode-pumped solid-state) laser 561 (single-track mode; 1 airy unit [a measure of pinhole radius size]; dual-band filter [500 to 545 band pass, 575 long pass]). Brightness and contrast were adjusted on complete images using ImageJ (68).

Cryofixation, chemical fixation, and transmission electron microscopy. Infected cells were cryofixed in an EM HPM100 high-pressure-freezing machine (Leica Microsystems, Vienna, Austria) (69) using cellulose capillary tubes (a kind gift from Heinz Schwarz) (70), Freeze substitution (Balzers FSU 010; Bal-Tec, Balzers, Liechtenstein) was performed as described by Leonidova et al. (71). Subsequently, samples were embedded in Epon resin (Fluka, St. Louis, MO, USA) or LR White resin (Electron Microscopic Sciences, Hatfield, PA, USA) as described by the manufacturers. Sections (70 nm) were examined using a CM100 transmission electron microscope (Philips, Eidhoven, Netherlands). For imaging, a Quemesa transmission electron microscopy (TEM) charge-coupled-device (CCD) camera and iTEM software v 5.1 (both from Olympus Soft Imaging Solutions, Münster, Germany) were used.

For chemical fixation, infected cells were fixed with 2% glutaraldehyde (GA) and 1% PFA in HL5-C for 2 h at room temperature. Subsequently, the cells were postfixed with 2% GA-sodium cacodylate (0.1 M) and finally stained with 2% OsO_4 and 1.5% $K_3Fe(CN)_6$. Before dehydration with ethyl alcohol (EtOH), samples were stained with 1.5% uranylacetate for 30 min. Finally, the cell pellets were embedded in Epon, and sections were prepared and examined as described above for cryofixed samples (for a detailed description of the method, see the supplemental material).

Zebrafish embryo maintenance. Zebrafish (*Danio rerio*) AB wt embryos were obtained from the Zebrafish Laboratory facility at the Norwegian University of Life Science. The embryos were dechorionated manually at 30 h postfertilization, transferred to fresh embryo water, and kept at 28°C before injections. All embryos were kept at 22°C after injections, and the water was changed at least every second day. Phenyl-2-thiourea (PTU) (Sigma-Aldrich, St. Louis, MO, USA) was added to the embryo water to a concentration of 0.003% (wt/vol) to reduce pigmentation for imaging purposes.

Zebrafish embryo microinjections. Preparation of bacteria and intravascular microinjections of 1 nl into the duct of Cuvier were performed as described previously (46). The *F. noatunensis* subsp. *noatunensis* wt and Δ*iglC* strains used for zebrafish embryo microinjections expressed GFP in *trans*, and *F. noatunensis* subsp. *noatunensis* Δ*iglC*$^{+}$ expressed IglC in *trans*. The number of injected CFU was determined by plating 10-fold serial dilutions from the injection solution, as described previously (46), and was found to be 2.2×10^3 to 3.5×10^3 CFU per injection. A control group was injected with sterile PBS (pH 7.4). Each group consisted of at least 30 embryos. Two embryos per group were imaged on days 2, 4, and 6 postinjection according to the protocol described for the Leica DM IRB (46). Samples for DNA extraction (see below) were taken at 3 and 7 days postinfection (dpi). The experiment was terminated at 7 dpi.

Sampling and DNA extraction from zebrafish embryos and *Dictyostelium*. On days 3 and 7, zebrafish embryos (12 from each group) were euthanized with an overdose of tricain (200 to 300 μg/ml), after which they were split into samples consisting of three embryos per tube, the liquid was replaced with 200 μl RNALater, and the samples were stored at 4°C until DNA extraction. For isolation of genomic DNA from *Dictyostelium*, 5×10^6 cells were collected at appropriate time points and stored at −20°C. Genomic DNA was extracted with a Qiagen DNeasy blood and

tissue kit (Qiagen, Venlo, Netherlands) according to the protocol for animal tissues (spin column protocol).

***Francisella*-specific quantitative PCR.** Five microliters of gDNA was used as the template for qPCR in a 20-μl reaction mixture using LightCycler 480 SYBR green I Master mix (Roche, Basel, Switzerland) and a Lightcycler 480 qPCR machine (Roche) according to the manufacturer's instructions. Samples were run in duplicate, and samples from 5 *Dictyostelium* infection experiments were used for quantification via qPCR. *F. noatunensis* subsp. *noatunensis*-specific primers (see Table S1 in the supplemental material, Q9 and Q10) for quantification of *F. noatunensis* subsp. *noatunensis* genomes were obtained from Duodu et al. (72). *F. noatunensis* subsp. *noatunensis*, genome equivalents were obtained by normalization of the *F. noatunensis* subsp. *noatunensis*-specific gene to *Dictyostelium rnlA* as a reference gene (73). *Dictyostelium* cell growth was included by multiplying *F. noatunensis* subsp. *noatunensis* genome equivalents by the *Dictyostelium* growth factor. For zebrafish experiments, 1 ng *F. noatunensis* subsp. *noatunensis* gDNA was used as an equilibrator in the qPCR run, and absolute quantification was performed so that 20 fg corresponded to 10 *F. noatunensis* subsp. *noatunensis* genome equivalents, as described previously (72).

RT-PCR of autophagy-associated genes. For reverse transcription (RT)-PCR analysis of *atg8* and *p62*, *F. noatunensis* subsp. *noatunensis* wt-infected and mock-treated cells were lysed with TRIzol (Life Technologies, Carlsbad, CA, USA) at the indicated time points. RNA extraction was performed using the PureLink RNA minikit (Life Technologies) according to the manufacturer's instructions for TRIzol extraction. For subsequent cDNA synthesis, the Maxima First Strand cDNA synthesis kit (Thermo Scientific, Waltham, MA, USA) was used according to the manufacturer's instructions. The cDNA was diluted 1:10 in nuclease-free water, and 5 μl of each sample was used as the template in an RT-PCR with the same setup and machine as described for *Francisella*-specific qPCR. Primers for *GAPDH*, *atg8*, and *p62* are listed in Table S1 in the supplemental material. Samples were run in duplicate, and samples from 4 *F. noatunensis* subsp. *noatunensis* wt infection experiments were analyzed. The resulting data were analyzed using the $\Delta\Delta C_T$ method with *gapdh* as a reference gene.

RESULTS

***Dictyostelium* does not feed on *F. noatunensis* subsp. *noatunensis*.** To monitor whether *Dictyostelium* can use *Francisella* as a food source, we examined *Dictyostelium* growth on a lawn of bacteria using the plaque assay, as established by Cosson et al. (54). When seeded on a dense lawn of nonpathogenic *Klebsiella aerogenes*, *Dictyostelium* cells were able to grow and form plaques (Fig. 1A) after 4 days. In contrast, *Dictyostelium* was not able to form plaques when placed on a lawn of *F. noatunensis* subsp. *noatunensis* wt bacteria (Fig. 1B). These observations suggest that *Dictyostelium* is not able to utilize *Francisella* as a nutrient source, in contrast to food bacteria, like *Klebsiella*. As with other pathogenic bacterial species, this could result from bacterial evasion of the degradative phagosomal maturation pathway (55).

***Francisella* persists and replicates in *Dictyostelium*.** *Dictyostelium* cells were allowed to ingest GFP-expressing *F. noatunensis* subsp. *noatunensis* wt bacteria in a synchronous fashion, and subsequently, the number of bacteria per *Dictyostelium* cell was monitored up to 48 hpi (Fig. 1C). Manual counting of the bacterial load per single cell using fluorescence microscopy revealed that the percentage of infected cells decreased gradually from 86.2% (1 hpi) to 11.7% (48 hpi). In the early phase of the infection, until 6 hpi, the proportion of cells containing more than 3 bacteria decreased from 53.1% to 20.3% infected cells. However, in the late phase (24 to 48 hpi) the proportion of cells with more than 3 bacteria increased to 32.2% (24 hpi) and 36.7% (48 hpi), respectively (Fig. 1C). Taking into account that *Dictyostelium* and *Francisella* possess similar generation times of approximately 8 h in culture (62, 74), these data indicate that the total number of bacteria starts to increase at 24 hpi.

The *Francisella* virulence factor IglC has been shown to be an essential bacterial factor to escape phagosomal maturation (33, 75), which is crucial for bacterial persistence in the host cell. *iglC* is located in the *iglABCD* locus (Fig. 1D) within the FPI, which displays the highest similarity to those of *F. philomiragia* (~96% identity) and *F. noatunensis* subsp. *orientalis* (88% to 96.7%). The *igl* sequence identity between *F. noatunensis* subsp. *noatunensis* and the *F. tularensis* lineage ranges from 81.1% to 85.8% (Fig. 1D; see Fig. S1 in the supplemental material). We generated an *F. noatunensis* subsp. *noatunensis iglC* knockout strain (Δ*iglC*) and compared the fate of this mutant to that of wt bacteria in *Dictyostelium* cells (Fig. 1C and E). The initial loads of bacteria per cell were very similar for *F. noatunensis* subsp. *noatunensis* wt and Δ*iglC* at 1 hpi (85.6 and 84.6%, respectively). In contrast to the wild type, the number of infected cells, as well as the number of Δ*iglC* bacteria per cell, dropped rapidly at 4 hpi (wt, 64.2%; Δ*iglC*, 13%). Eventually, intracellular Δ*iglC* bacteria almost disappeared from the *Dictyostelium* culture, indicated by low infection rates at 24 (3.5%) and 48 (0.6%) hpi. Surprisingly, the plaque assay revealed that amoebae were not able to grow on a lawn of the Δ*iglC* strain (not shown).

In addition to quantitative fluorescence microscopy of single cells, we applied flow cytometry analysis, which allowed us to quantitatively analyze the fluorescence of a large number of cells at different time points (see Fig. S2 in the supplemental material). As indicated by the bacterial count using microscopy, flow cytometry analysis revealed that *Dictyostelium* cells infected with wt *Francisella* showed a 2-fold increase in fluorescence over time, indicating growth of GFP-expressing *F. noatunensis* subsp. *noatunensis* (Fig. 1F). In contrast, the green fluorescent signal of the Δ*iglC* mutant showed a decrease to 13% at 4 hpi and remained low until 48 hpi.

In addition to these visual analyses, we used quantitative PCR to establish the number of *Francisella* genomes in relation to host cell genomes at the indicated time points (Fig. 1G). Overall, the results confirmed what had been observed with the previous approaches. The number of *F. noatunensis* subsp. *noatunensis* wt genomes increased, after an initial reduction at 4 hpi by 2.3-fold, until 48 hpi. In contrast, when cells infected with *F. noatunensis* subsp. *noatunensis* Δ*iglC* bacteria were analyzed, the number of genomes decreased rapidly, suggesting complete clearance of the bacteria. Taking into account that *Francisella* bacteria were not able to grow in *Dictyostelium* growth medium, these observations suggest that wt bacteria are able to infect and replicate within their *Dictyostelium* host cells in an IglC-dependent manner.

The attenuation of *F. noatunensis* subsp. *noatunensis* Δ*iglC* bacteria was further confirmed in a multicellular organism using the zebrafish embryo model established by Brudal et al. (46). Microinjections of *F. noatunensis* subsp. *noatunensis* were administered intravenously into the duct of Cuvier (see Fig. S3A in the supplemental material), and the course of infection was monitored by fluorescence microscopy (see Fig. S3B to G in the supplemental material) and *F. noatunensis* subsp. *noatunensis*-specific qPCR (see Fig. S3H in the supplemental material). Both methods showed a lower mean bacterial burden in the Δ*iglC* group than in the wt group on day 3 and day 7 postinfection. The wt-infected zebrafish embryos were clinically observed through notably re-

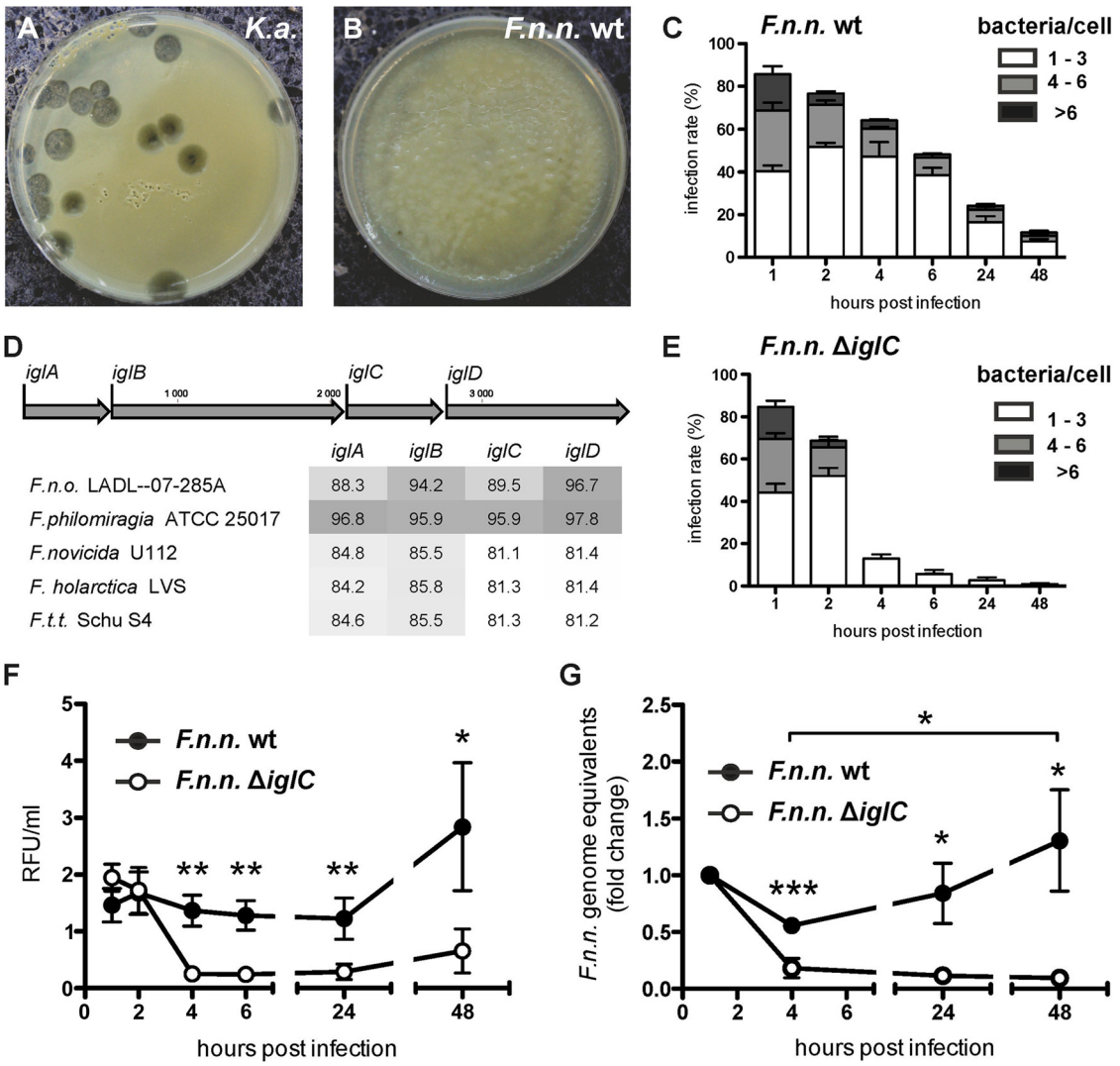

FIG 1 Persistence and replication of *F. noatunensis* subsp. *noatunensis* in *Dictyostelium* is dependent on IglC. (A and B) Plaque assay to determine resistance of bacteria to feeding of *Dictyostelium*. *Dictyostelium* feeds and forms plaques on a lawn of *K. aerogenes* (*K.a.*) (A), but not on *F. noatunensis* subsp. *noatunensis* (*F.n.n.*) wt (B). Shown are images of one representative experiment ($n = 3$). (C and E) Infection rate (*y* axis) and bacteria/cell (bar sections) of *F. noatunensis* subsp. *noatunensis* wt (C) and Δ*iglC* (E) in *Dictyostelium* wt cells over 48 hpi. Data were collected from 7 replicates, and a minimum of 100 cells were counted. The error bars indicate standard errors of the mean (SEM). (D) Nucleotide sequence comparison of *iglA* to *iglD* in *F. noatunensis* subsp. *noatunensis* FSC769 with other selected *Francisella* spp. (*F.t.t.*, *F. tularensis* subsp. *tularensis*; *F.n.o.*, *F. noatunensis* subsp. *orientalis*). The results are presented as percent nucleotide identity with the *iglA* to *iglD* loci of *F. noatunensis* subsp. *noatunensis* FSC769 after pairwise comparison. The depth of gray shading indicates the level of sequence identity, with dark gray representing the highest similarity. (F and G) Bacterial replication of *F. noatunensis* subsp. *noatunensis* wt and Δ*iglC* was measured by flow cytometry analysis of bacterial green fluorescence per unit volume of infected cell culture (F) and by qPCR of *F. noatunensis* subsp. *noatunensis* genomes normalized to host cell genomes (G). Data from 8 (F) and 5 (G) independent experiments (means ± SEM) were collected (unpaired, two-tailed *t* test; *, $P < 0.05$; **, $P < 0.01$; ***, $P < 0.001$).

duced flight reaction (unpublished observation) compared to the other groups. All infected groups showed an increase in bacterial load from days 3 to 7, but the total number of *F. noatunensis* subsp. *noatunensis* genomes on day 7 was considerably lower in the Δ*iglC* group. This experiment shows that *F. noatunensis* subsp. *noatunensis* Δ*iglC* growth is also restricted in zebrafish embryos. The *F. noatunensis* subsp. *noatunensis* Δ*iglC* mutant expressing IglC in *trans* (*iglC*$^+$) partly regained wt growth performance in the embryos.

***Francisella* avoids phagosomal maturation in *Dictyostelium* in an IglC-dependent way.** The phagosomal escape of *Francisella* is IglC dependent, and it is well established that escape from phagosomal maturation is a prerequisite for successful infection of *Francisella* (14, 17, 33, 63). Therefore, we quantified the association of wt and Δ*iglC F. noatunensis* subsp. *noatunensis* with established phagosomal maturation markers (55) over time using immunofluorescence microscopy. p80 is a putative *Dictyostelium* copper transporter that is enriched on phagosomes toward the late maturation stage (65). Both *Francisella* strains showed strong accumulation of p80 at the early stage (67% of wt and 79% of Δ*iglC* at 1 hpi); however, over the course of infection, the association of p80 with wt bacteria fell to 4% at 48 hpi (Fig. 2A and B). In contrast, p80 association with *Francisella* bacteria lacking *iglC* remained high (from 79 to 68%) over 48 h.

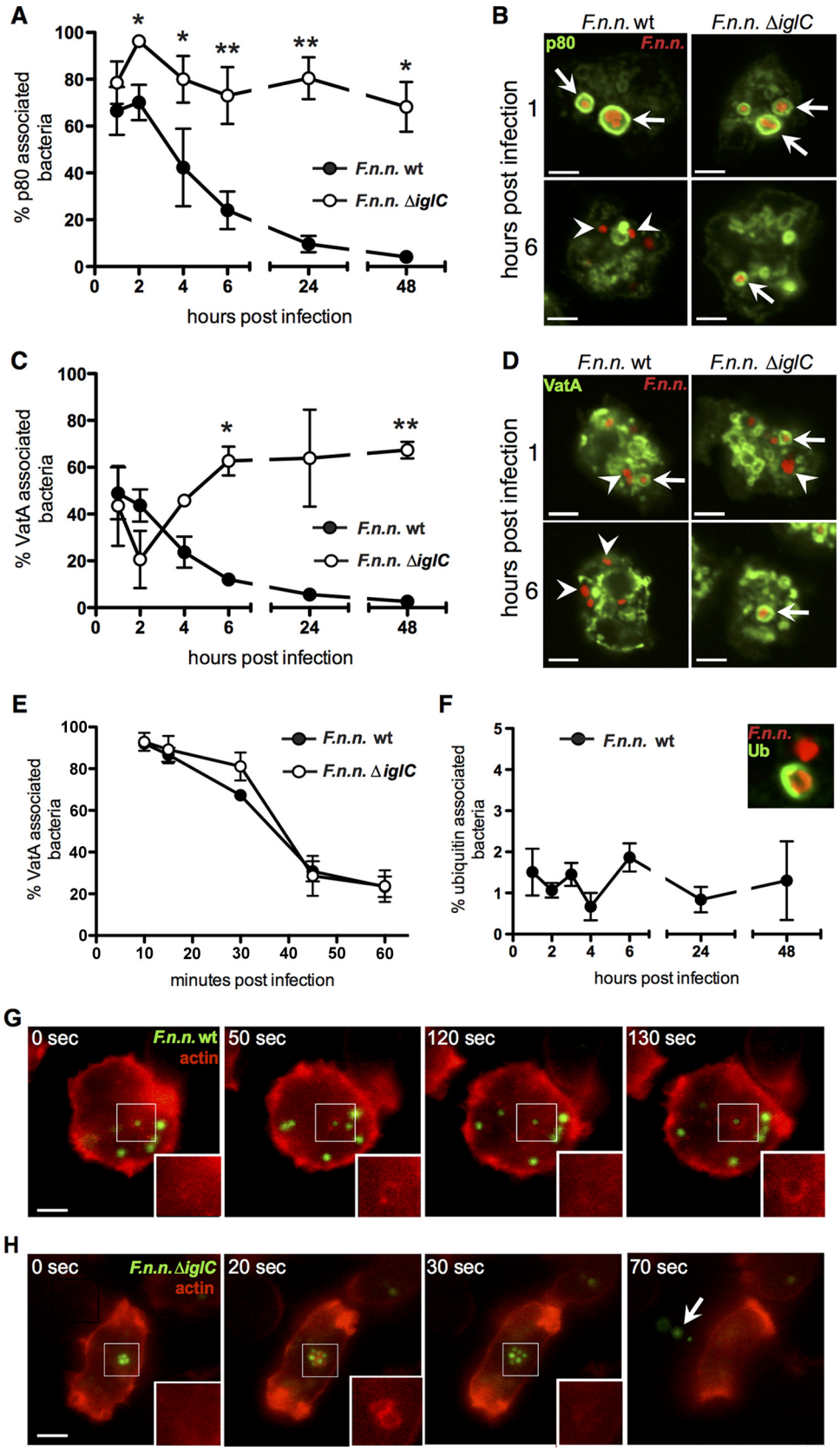

FIG 2 Escape from phagosomal maturation by *F. noatunensis* subsp. *noatunensis* is dependent on IglC. (A) Association rates of *F. noatunensis* subsp. *noatunensis* (*F.n.n.*) wt and Δ*iglC* with the endosomal marker p80 over 48 hpi (means ± SEM; $n = 3$ or 4). (C and E) Association rates of *F. noatunensis* subsp. *noatunensis* wt and Δ*iglC* with the acidification marker VatA over 48 hpi (C) and early in infection (≤1 hpi) (E). (B and D) Corresponding micrographs of p80 (green)

We also followed the association of bacteria with VatA (Fig. 2C to E), the cytosolic and catalytic subunit of the V-ATPase (76). The presence of VatA on the vacuole containing bacteria is an indication that bacteria are present in an acidic, potentially bactericidal compartment (77). Wt and Δ*iglC Francisella* showed equal associations of more than 90% in VatA-positive compartments at 15 min postinfection, which dropped similarly for both strains until 1 hpi (Fig. 2E). Contrasting with the constant drop in association observed for wt bacteria, the VatA association of Δ*iglC* bacteria continued to fall only until 2 hpi and subsequently increased to 63% (6 hpi) and then remained stable. After phagocytosis, VatA was retrieved from the vacuoles containing bacteria in both strains and followed typical VatA dynamics in *Dictyostelium* (78), but only wt bacteria were able to escape the VatA-positive compartment permanently (Fig. 2C and D). In contrast, the Δ*iglC* mutant regained its VatA accumulation by either reassociation or reinfection. Taken together, the observed patterns suggest that *F. noatunensis* subsp. *noatunensis* wt bacteria are able to escape phagosomal maturation. Without IglC, the bacteria fail to escape and remain within the degradative maturation pathway.

Francisella bacteria are known to translocate very early in infection from their phagosome into the host cell cytosol in an IglC-dependent fashion (18, 33, 75). Therefore, we quantified the colocalization of *Francisella* bacteria with ubiquitin. Ubiquitination occurs only if bacteria are accessible to the host cell cytosol. Associations were counted using fluorescence microscopy with fixed samples at the indicated time points. In contrast to the wild type, which showed a stable ubiquitin association with 1 to 2% of the bacteria (Fig. 2F), no association was observed with the mutant strain lacking IglC.

Finally, in *Dictyostelium*, phagosomal maturation ends with exocytosis of the ingested particle or bacterium (79). In general, exocytosis is accompanied by a burst of F actin accumulation around the particle (78). Therefore, we infected *Dictyostelium* cells expressing a red fluorescent actin marker (Lifeact-RFP) (80) with green fluorescent *Francisella* and used live fluorescence microscopy to follow their fate. Wt *F. noatunensis* subsp. *noatunensis* was observed to be evenly distributed within the host cell and showed only occasional, transient association with F actin (Fig. 2G; see Movie S1 in the supplemental material). In contrast, Δ*iglC* bacteria were found to be clustered in compartments and more frequently exocytosed, accompanied by a sudden flash of F actin (Fig. 2H; see Movie S2 in the supplemental material). These results support the model that, as in other host systems with various *Francisella* strains (33, 63, 75), *F. noatunensis* subsp. *noatunensis* escapes the early phagosome in an IglC-dependent fashion into the cytosol of *Dictyostelium*, where it replicates.

Electron microscopic analyses reveal cytosolic *Francisella*. To confirm the subcellular localization of *Francisella* bacteria within *Dictyostelium* cells, ultrastrucural analysis was performed at 1, 4, and 24 hpi. Samples were either chemically fixed and processed by conventional room temperature dehydration or cryofixed with high-pressure freezing (HPF) and processed by freeze substitution in order to improve the ultrastructural preservation. With both methods, at 1 hpi, both *F. noatunensis* subsp. *noatunensis* wt and Δ*iglC* resided within vacuoles with well-defined membranes (HPF, Fig. 3A, B, E, and F; chemical fixation, see Fig. S4A in the supplemental material). In addition, in the cryofixed samples, ruptured phagosomal membranes were observed for *F. noatunensis* subsp. *noatunensis* wt (see Fig. S5A and B in the supplemental material), but not with the Δ*iglC* mutant strain. Similar events were also observed by fluorescence microscopy, in which *F. noatunensis* subsp. *noatunensis* wt bacteria were seen escaping a rupturing p80-positive compartment at 4 hpi (see Fig. S5C and D in the supplemental material). At 4 and 24 hpi, most *F. noatunensis* subsp. *noatunensis* wt bacteria were localized within the *Dictyostelium* cytosol without a surrounding membrane (Fig. 3C and D; see Fig. S4B in the supplemental material). In contrast to wt bacteria, *F. noatunensis* subsp. *noatunensis* Δ*iglC* bacteria were located in vacuoles at 4 hpi as either single, multiple, or often partly digested bacteria (Fig. 3G). In chemically fixed samples, bacteria, both phagosomal and cytosolic, were surrounded with electron-translucent areas, so-called halos (see Fig. S4A and B in the supplemental material), which were previously suggested to represent a bacterial capsule (17, 22). However, in cryofixed samples, we could observe an electron-pale area only around cytosolic bacteria (Fig. 3). This area represented weakly contrasted material and looked notably different from the halos around chemically fixed bacteria. Lectins specific for mannose, galactose, glucose, *N*-acetylgalactosamine, *N*-acetylglucosamine, or sialic acid-containing carbohydrates did not bind to this electron-pale zone (data not shown). At all stages, we observed great variations of the bacterial structure, from round to starlike shapes, in chemically as well as cryo-fixed samples, indicating that these shapes were not artifactual.

***Francisella* associates with autophagic markers.** Pathogenic bacteria present in the host cell cytosol are known to interact with the autophagic pathway of the host cell (81); however, for *Francisella*, these interactions are disputed (21, 24, 25). To complement current concepts and to gain further insight, we investigated the interaction of *F. noatunensis* subsp. *noatunensis* with the autophagic machinery in our system. We infected *Dictyostelium* cell lines expressing one of the following GFP-tagged proteins with *F. noatunensis* subsp. *noatunensis* wt expressing mCherry: ubiquitin, which labels substrates for autophagic degradation; p62, a ubiquitin scaffolding protein; or Atg8, which is required for the formation of autophagosomal membranes. The association of bacteria with the respective marker protein was quantified via live-cell fluorescence microscopy (Fig. 4A to D). During the early phase of infection (1 to 6 hpi), the association of bacteria with the marker proteins remained below 3%. At the late stage of infection (24 hpi), the associations with ubiquitin and p62 rose to 5 and 9%, respectively. In contrast, the association with Atg8 remained at a low but constant level (1 to 2%) throughout infection. Electron microscopy on HPF sections revealed that formerly cytosolic *F.*

association with *F. noatunensis* subsp. *noatunensis* (red) wt and Δ*iglC* at 1 and 6 hpi. Three independent experiments were conducted for each time course, with representative micrographs at 1 and 6 hpi. (F) Ubiquitin (Ub) association of *F. noatunensis* subsp. *noatunensis* wt over 48 h (means ± SEM; $n = 3$ or 4). The inset shows ubiquitin-positive (green) and -negative (red) examples of *F. noatunensis* subsp. *noatunensis* wt. Ubiquitinated Δ*iglC* bacteria were not detected. A minimum of 100 bacteria were counted for association studies. (G and H) Time frames of *Dictyostelium* Lifeact-RFP cells (red) infected with GFP-expressing *F. noatunensis* subsp. *noatunensis* wt (green) at 18 hpi (G) and Δ*iglC* at 2 hpi (H). The areas of interest are boxed, and the insets show the red channels of the regions of interest. In panels B and D, the arrows indicate marker-positive compartments and the arrowheads indicate marker-negative bacteria; in panel H, the arrow indicates exocytosed bacteria. Scale bars, 5 μm. Unpaired, two-tailed *t* test: *, $P < 0.05$; **, $P < 0.01$.

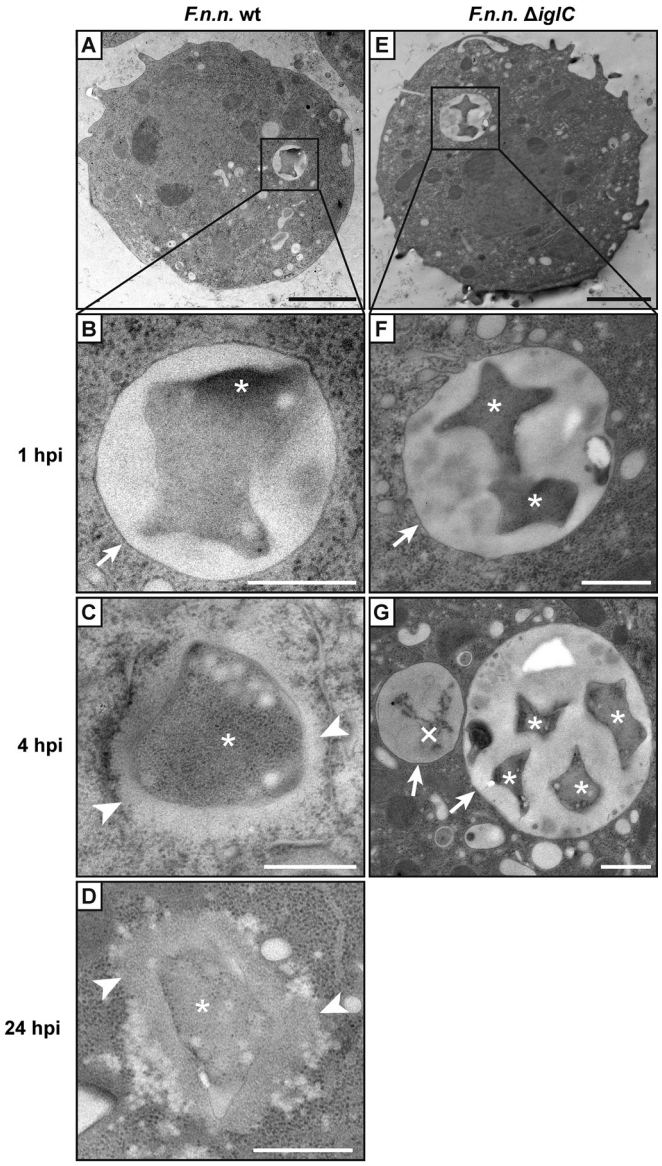

FIG 3 Cytosolic translocation of *F. noatunensis* subsp. *noatunensis* is dependent on IglC. Ultrastructural analysis of high-pressure-frozen *Dictyostelium* wt cells infected with *F. noatunensis* subsp. *noatunensis* (*F.n.n.*) wt (A to D) and Δ*iglC* (E to G) was performed. Shown are representative examples of overviews (A and E) and high-magnification images at 1 (B and F), 4 (C and G), and 24 (D) hpi. *, intact *F. noatunensis* subsp. *noatunensis*; ×, digested *F. noatunensis* subsp. *noatunensis*; arrows, membranes enclosing bacteria; arrowheads, electron-pale areas characteristic of *F. noatunensis* subsp. *noatunensis* after HPF. Scale bars, 2 μm (A and E) and 500 nm (B to D, F, and G).

noatunensis subsp. *noatunensis* wt bacteria were enclosed inside a vacuole, which in addition contained ribosomal structures and could therefore represent autophagosomes (see Fig. S4C and D in the supplemental material).

mRNA levels of autophagic genes are slightly upregulated. To quantify activation of autophagy in infected *Dictyostelium* cells, we measured the amounts of mRNAs of selected host cell genes at different time points during infection by qRT-PCR (Fig. 4E). The amounts of *atg8* and *p62* mRNA were compared to a mock control (uninfected cells). Infected *Dictyostelium* wt cells showed slightly increased (1.5- to 2-fold) *atg8* mRNA levels compared to the mock control in the early phase of infection; however, it was significant only at 2 and 6 hpi. In the late phase, from 24 to 48 hpi, *atg8* mRNA levels dropped to levels similar to those observed for the mock control. The amount of *p62* mRNA was slightly elevated at 6 and 24 hpi.

Increased bacterial burden in *Dictyostelium* cells lacking functional Atg1. Analyses of cellular markers and mRNA levels argue for activation of the autophagic pathway by *F. noatunensis* subsp. *noatunensis* in the *Dictyostelium-Francisella* system. To investigate the impact of autophagy on the outcome of infection, we monitored *Francisella* infection in *Dictyostelium atg1* knockout cells (Δ*atg1*) (57). Atg1 (Ulk1/2) is a key component of the canonical autophagy initiation complex, and the *Dictyostelium* Δ*atg1* mutant is strictly impaired in autophagy (82).

Fluorescence microscopy was used to establish the number of bacteria in *Dictyostelium* Δ*atg1* cells (Fig. 4F). In the early phase of infection (up to 6 hpi), wt *F. noatunensis* subsp. *noatunensis* followed similar courses of infection for wt and Δ*atg1* host cells, with gradually decreasing infection rates and bacterial burden per cell. However, at a late stage, Δ*atg1* host cells showed a significantly higher infection rate at 24 (wt, 24.2%; Δ*atg1*, 37.6%) and 48 (wt, 11.7%; Δ*atg1*, 23.5%) hpi and more bacteria per cell than *Dictyostelium* wt cells (Fig. 1D). In addition to single-cell counting, we followed the infection by applying flow cytometry (Fig. 4G). The results agreed with the manual counting and revealed a significantly stronger increase of the bacterial burden in *Dictyostelium* Δ*atg1* cells than in the wt from 24 hpi onward.

***F. noatunensis* subsp. *noatunensis* shows a higher degree of ubiquitin association in Δ*atg1* cells.** The higher bacterial burden in the *Dictyostelium* Δ*atg1* mutant suggests that *F. noatunensis* subsp. *noatunensis* interacts with the autophagic machinery. To determine if there is a difference in the escape from phagosomal maturation when the autophagic machinery is impaired, we quantified the association of established phagosomal maturation markers with *F. noatunensis* subsp. *noatunensis* over the course of infection using fluorescence microscopy. The association of bacteria with p80, as well as VatA, showed no significant difference between *Dictyostelium* wt and Δ*atg1* cells (see Fig. S6A and B in the supplemental material). However, the association of bacteria with ubiquitin increased significantly in *Dictyostelium* Δ*atg1* cells, from 3% (6 hpi) to 27% (24 hpi) and eventually 51% at 48 hpi (see Fig. S6C and D in the supplemental material). Thus, the inital courses of infection (up to 6 hpi) are comparable in wt and Δ*atg1* host cells regarding phagosomal maturation and bacterial burden. In contrast, the late stage is characterized by a higher bacterial burden in Δ*atg1* cells, which is accompanied by an accumulation of ubiquitin-associated bacteria.

DISCUSSION

Our data reveal that *F. noatunensis* subsp. *noatunensis* infects *Dictyostelium* and that the course of infection recapitulates the infection of mammalian macrophages (Fig. 5A and B) (14, 17, 21, 33). As with other pathogenic bacteria (54, 83–86), *Dictyostelium* was not able to feed on a lawn of *F. noatunensis* subsp. *noatunensis*. The lack of growth on avirulent *F. noatunensis* subsp. *noatunensis* Δ*iglC* suggests either that IglC is not the only virulence factor that provides resistance against the amoeba or that *Dictyostelium* is in general unable to efficiently digest the bacteria.

F. noatunensis subsp. *noatunensis* is ingested via phagocytosis

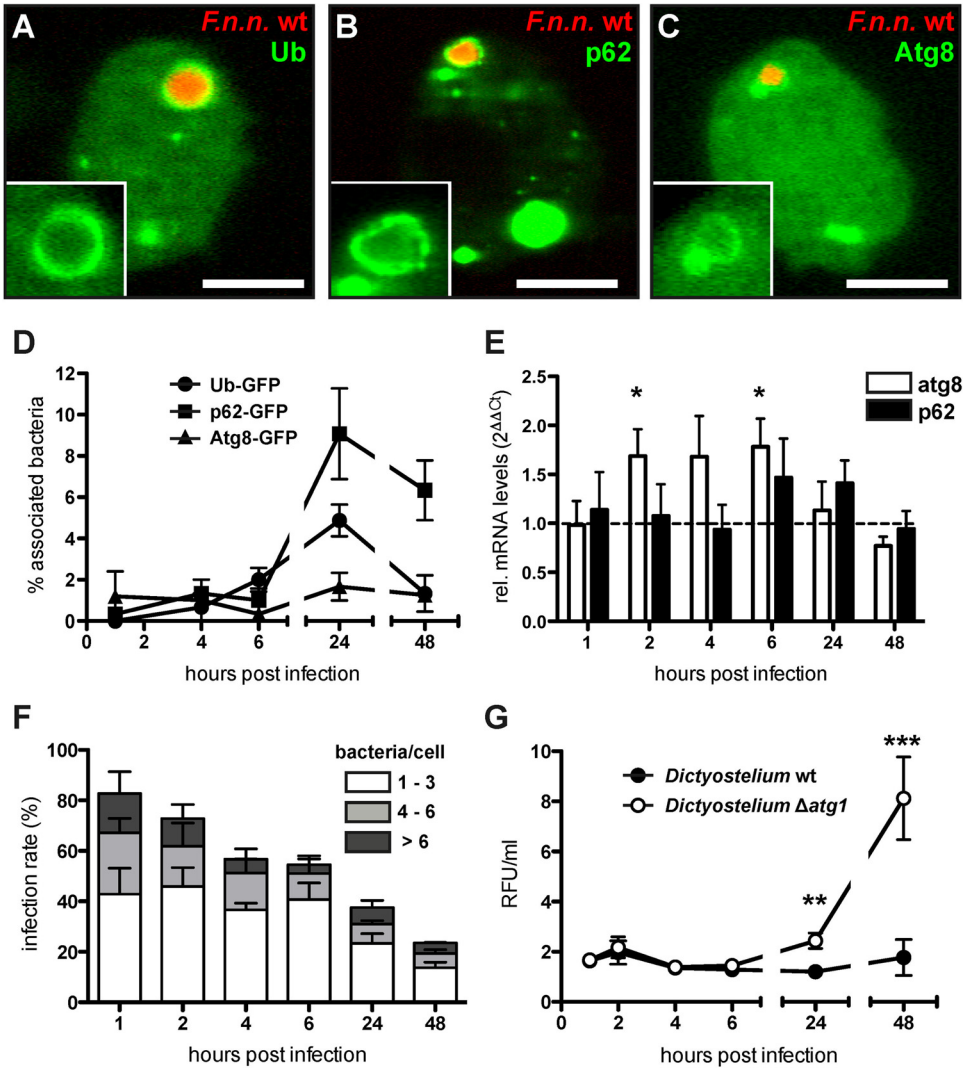

FIG 4 *F. noatunensis* subsp. *noatunensis* interacts with the autophagic machinery and shows increased growth in *Dictyostelium* Δ*atg1* cells. (A to C) *Dictyostelium* cells expressing GFP-tagged markers (green) of the autophagy machinery were infected with *F. noatunensis* subsp. *noatunensis* (*F.n.n.*) wt expressing mCherry (red). Shown are representative micrographs of a positive association of *F. noatunensis* subsp. *noatunensis* wt with ubiquitin (A), p62 (B), and Atg8 (C) at 24 hpi. Scale bars, 5 μm. (D) Association rates of *F. noatunensis* subsp. *noatunensis* wt with autophagy markers over 48 hpi (means ± SEM; $n = 3$ or 4). (E) *p62* and *atg8* mRNA levels were measured in *Dictyostelium* wt cells infected with *F. noatunensis* subsp. *noatunensis* wt via RT-PCR over 48 hpi. The mRNA amounts of the genes were normalized to *gapdh* as a housekeeping gene and are displayed as the fold change (means and SEM; $n = 4$). (F) Infection rate and numbers of bacteria per cell of *Dictyostelium* Δ*atg1* cells infected with *F. noatunensis* subsp. *noatunensis* wt over 48 hpi (mean and SEM; $n = 3$). (G) Bacterial growth in *Dictyostelium* wt and Δ*atg1* cells was measured by flow cytometry analysis and is displayed in RFU per unit volume of cell culture (means ± SEM; $n = 6$ to 13) (unpaired, two-tailed *t* test; *, $P < 0.05$; **, $P < 0.01$; ***, $P < 0.001$).

by *Dictyostelium* and initially resides in a *de novo*-formed phagosome. Subsequently, as with *F. tularensis* in other host cells (14, 17, 18, 25, 33), *F. noatunensis* subsp. *noatunensis* bypasses phagosomal maturation and escapes into the cytosol (Fig. 5) (14, 17, 18, 25, 33). *F. tularensis* has been shown to associate with early and late endosomal markers and escapes the phagosome in mammalian cells at the early stage of infection (1 to 8 hpi) (17, 18, 25, 33). This time correlates with the observed cytosolic translocation in *Dictyostelium*, as monitored by the association of wt *F. noatunensis* subsp. *noatunensis* with p80 and electron microscopy analyses. Similar to *F. tularensis* (21), the association of *F. noatunensis* subsp. *noatunensis* with ubiquitin confirms the bacterial presence in, or accessibility to, the cytosol in *Dictyostelium*. The low number of associations could be due either to a constant turnover of ubiquitin (87) or, possibly, to the shedding of bacterial outer proteins acting as a decoy for the host cell, as has been described for mycobacteria (88).

The escape from phagosomal maturation in *Dictyostelium* is dependent on the *Francisella* virulence factor IglC. In contrast to the *F. noatunensis* subsp. *noatunensis* wt, the *iglC* deletion mutant follows the classical phagosomal maturation pathway, as described for latex beads or nonvirulent bacteria in *Dictyostelium* (51, 78, 89) that remain within an endosomal compartment with no colocalization with ubiquitin. Eventually, the bacteria are exocytosed, as observed by live microscopy.

A major hallmark of phagosomal maturation is the acidifica-

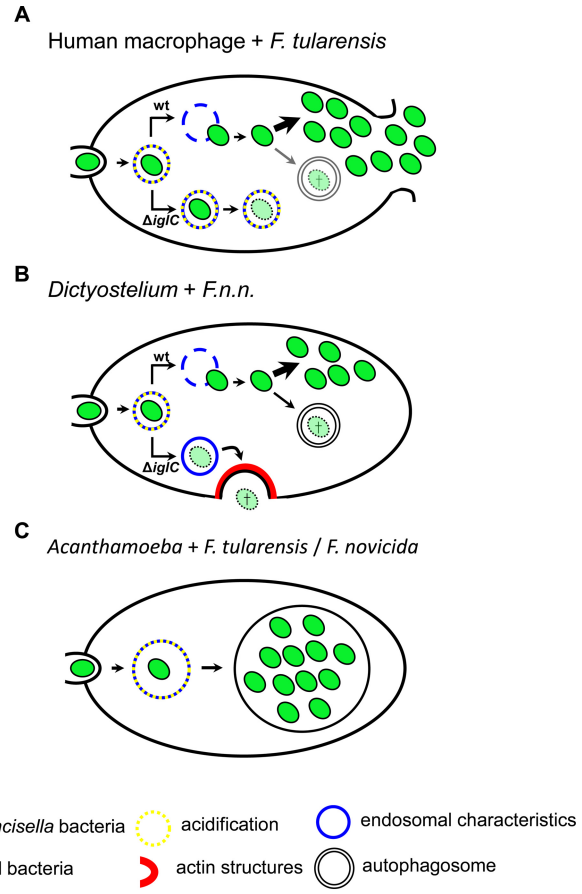

FIG 5 Comparison of *Francisella* infections in human, *Dictyostelium*, and an environmental amoeba. (A and B) Macrophages (A) and *Dictyostelium* (B) phagocytose *Francisella* bacteria, forming a phagosomal compartment with endosomal characteristics. With acidification of this compartment, *Francisella* wt bacteria escape the phagosome into the cytosol early in infection. Avirulent mutant bacteria (Δ*iglC*) remain within the phagosome (which is reneutralized in *Dictyostelium*) but are either attenuated in growth (macrophages) or exocytosed (*Dictyostelium*). In both host cells, *Francisella* replicates in the cytosol, and a small proportion of bacteria are targeted by autophagy. (C) In *Acanthamoeba*, a potential environmental host, the course of *Francisella* infection is very different. After phagocytosis, *Francisella* resides in a spacious vacuole showing endosomal properties and acidification. In contrast to macrophages and *Dictyostelium*, *Francisella* subsequently does not escape its compartment but replicates inside the vacuole. Intriguingly, cells infected with *F. novicida* show cyst formation. *F.n.n.*, *F. noatunensis* subsp. *noatunensis*.

tion of the newly formed phagosome. Previous studies showed transient acidification of the *F. tularensis*-containing phagosome in the early phase of infection, but its impact on the course of infection is disputed (14, 15, 32). The *F. noatunensis* subsp. *noatunensis*-containing phagosome in *Dictyostelium* associates with the V-ATPase subunit VatA, suggesting acidification. The virulence factor IglC has been associated with a protective role against acidification (63). However, the apparently *iglC*-independent VatA association observed in *Dictyostelium* suggests that avoidance of acidification occurs by escape from the phagosome (17, 63) rather than by active regulation.

The increase of *F. noatunensis* subsp. *noatunensis* bacteria in *Dictyostelium* starts in the late phase of infection and coincides with bacterial presence in the cytosol. This is in accordance with our zebrafish model system, which revealed an intracellular generation time of 43 h for *F. noatunensis* subsp. *noatunensis* wt (62). Also, in *Dictyostelium*, the attenuated phenotype of *F. noatunensis* subsp. *noatunensis* Δ*iglC* recapitulates what is observed in mammalian cells, where Δ*iglC* bacteria are not able to replicate inside their restricted vacuoles (18, 75). The attenuation of *F. noatunensis* subsp. *noatunensis* Δ*iglC* in zebrafish embryos corroborates the *Dictyostelium* phenotype in a multicellular organism featuring an innate immune system. These observations sustain the concept of using *Dictyostelium* as a platform for *Francisella* mutant screening and characterization.

Our ultrastructural analyses of HPF *Dictyostelium* cells infected with *F. noatunensis* subsp. *noatunensis* confirm that *Francisella* bacteria are indeed extremely polymorphic and indicate that the electron-translucent area around bacteria in chemically fixed samples is a fixation artifact. For chemically fixed *F. tularensis* in macrophages, a similar zone has been suggested to represent a capsule made of the polysaccharide O antigen (22). Nevertheless, in HPF samples, cytosolic bacteria were surrounded with an electron-pale area, which appeared to contain weakly contrasted material. We could not label this area with multiple lectins, which indicates that it is not enriched in certain carbohydrates.

In contrast to *Dictyostelium*, *Francisella* infection of other amoebae, such as *A. castellani* and *H. vermiformis*, follows a very different course. In the latter amoebae, the bacteria are found to replicate intracellularly in vacuoles and do not seem to translocate into the host cell cytosol (3, 48). In *A. castellani*, frequent cyst formation was observed, which was induced by the bacteria and might contribute to long-term survival of *Francisella* in the environment (3, 48). This different life cycle of *Francisella* in *Dictyostelium* compared to other amoebae suggests that *Dictyostelium* does not play a role in environmental transmission (Fig. 5). Instead, the susceptibility of *Dictyostelium* to *F. noatunensis* subsp. *noatunensis* and features shared with the mammalian system highlight evolutionarily conserved factors and common mechanisms between *Dictyostelium* and mammalian phagocytes.

Francisella has been described as interacting with the autophagic machinery; however, the impact and relevance of this interaction on the course of infection are debated and vary between host cell types (21, 24, 25). In *Dictyostelium*, the complete autophagic pathway is fully conserved, and its genetic tractability allows the dissection of *F. noatunensis* subsp. *noatunensis* interaction with the autophagic machinery. In *Dictyostelium* Δ*atg1* cells, *F. noatunensis* subsp. *noatunensis* growth is increased, which is not caused by drastically altered phagosomal maturation, but rather, coincides with bacterial association with autophagy markers. This suggests a degradative role for autophagy in the *Dictyostelium*-*F. noatunensis* subsp. *noatunensis* system. Also, in Atg5$^{-/-}$ murine embryonic fibroblasts lacking canonical autophagy, the bacterial burden of *F. tularensis* was increased, reflecting the protective role of autophagy in *Francisella* infection (24). However, this was not the case in Atg5$^{-/-}$ murine bone marrow-derived macrophages (21), thus highlighting the cell-type-specific role of autophagy in *Francisella* infection. In addition, *Francisella* infection of wt *Dictyostelium* cells was accompanied by increased levels of *p62* and *atg8* mRNA in the early phase of infection and decreased *atg8* mRNA levels at 48 hpi. Overall, this indicates a dynamic interaction with the autophagic machinery that is dependent on the time during infection.

Altogether, we demonstrated that *F. noatunensis* subsp. *noatunensis* passes through a course of infection in *Dictyostelium*

comparable to that of *F. tularensis* in macrophages, including the effect of the bacterial virulence factor IglC and interaction with autophagy as a host defense mechanism. Further highlighting the power of this model organism, *Dictyostelium* provides a wide range of genetic and chemical tools that can be used to facilitate a detailed dissection of host-pathogen interactions (51, 90). Therefore, the *Dictyostelium-Francisella* system is an excellent addition to current models of *Francisella* infection and expands our repertoire of tools to uncover the principles of virulence and host cell defense mechanisms.

ACKNOWLEDGMENTS

We thank Anne-Lise Rishovd for excellent qPCR work, Hendrik Herrmann for electron microscopy of chemically fixed samples, Frauke Bach for primer design, Ana C. S. Tavara for zebrafish supply, and Espen Brudal for zebrafish embryo microinjection expertise. We thank the Electron Microscopy Laboratory at the Department of Biosciences, University of Oslo, for access to the instruments and Tove Bakar for embedding of chemically fixed samples. We are thankful to Andreas Brech, Institute for Cancer Research, Oslo University Hospital, for his help with cryofixation; to Heinz Schwarz, Max Planck Institute for Developmental Biology, Tuebingen, Germany, and to Andres Kaech, University of Zurich, for discussions on high-pressure freezing and freeze substitution; and to Tone Aksnes Lian for technical assistance with cryofixation. This work would not have been possible without dictyBase (91).

FUNDING INFORMATION

University of Oslo provided funding to Elisabeth O. Lampe and Hanne C. Winther-Larsen. Prime Minister Gunnar Knudsen and wife Sofie, Barrister Per Ryghs legate, Kristine Bonnevies travel grant, and MLSUiO provided funding to Elisabeth O. Lampe. Deutsche Forschungsgemeinschaft (SPP1580) provided funding to Monica Hagedorn and Gareth Griffiths under grant number HA3474761. DAAD/Research Council of Norway provided funding to Hanne C. Winther-Larsen and Monica Hagedorn under grant number 225295.

The funders had no role in study design, data collection and interpretation, or the decision to submit the work for publication.

REFERENCES

1. **Abd H, Johansson T, Golovliov I, Sandström G, Forsman M.** 2003. Survival and growth of Francisella tularensis in Acanthamoeba castellanii. Appl Environ Microbiol **69:**600–606. http://dx.doi.org/10.1128/AEM.69.1.600-606.2003.
2. **Keim P, Johansson A, Wagner DM.** 2007. Molecular epidemiology, evolution, and ecology of Francisella. Ann N Y Acad Sci **1105:**30–66. http://dx.doi.org/10.1196/annals.1409.011.
3. **Santic M, Ozanic M, Semic V, Pavokovic G, Mrvcic V, Abu Kwaik Y.** 2011. Intra-vacuolar proliferation of F. novicida within H. vermiformis. Front Microbiol **2:**78. http://dx.doi.org/10.3389/fmicb.2011.00078.
4. **Foley JE, Nieto NC.** 2010. Tularemia. Vet Microbiol **140:**332–338. http://dx.doi.org/10.1016/j.vetmic.2009.07.017.
5. **Nylund A, Ottem KF, Watanabe K, Karlsbakk E, Krossøy B.** 2006. Francisella sp. (family Francisellaceae) causing mortality in Norwegian cod (Gadus morhua) farming. Arch Microbiol **185:**383–392. http://dx.doi.org/10.1007/s00203-006-0109-5.
6. **Sjödin A, Svensson K, Ohrman C, Ahlinder J, Lindgren P, Duodu S, Johansson A, Colquhoun DJ, Larsson P, Forsman M.** 2012. Genome characterisation of the genus Francisella reveals insight into similar evolutionary paths in pathogens of mammals and fish. BMC Genomics **13:**268. http://dx.doi.org/10.1186/1471-2164-13-268.
7. **Fortier AH, Slayter MV, Ziemba R, Meltzer MS, Nacy CA.** 1991. Live vaccine strain of Francisella tularensis: infection and immunity in mice. Infect Immun **59:**2922–2928.
8. **Oyston PC, Sjöstedt A, Titball RW.** 2004. Tularaemia: bioterrorism defence renews interest in Francisella tularensis. Nat Rev Microbiol **2:**967–978. http://dx.doi.org/10.1038/nrmicro1045.
9. **Colquhoun DJ, Duodu S.** 2011. Francisella infections in farmed and wild aquatic organisms. Vet Res **42:**47. http://dx.doi.org/10.1186/1297-9716-42-47.
10. **Hsieh CY, Tung MC, Tu C, Chang CD, Tsai SS.** 2006. Enzootics of visceral granulomas associated with Francisella-like organism infection in tilapia (Oreochromis spp.). Aquaculture **254:**129–138. http://dx.doi.org/10.1016/j.aquaculture.2006.03.044.
11. **Zerihun MA, Feist SW, Bucke D, Olsen AB, Tandstad NM, Colquhoun DJ.** 2011. Francisella noatunensis subsp. noatunensis is the aetiological agent of visceral granulomatosis in wild Atlantic cod Gadus morhua. Dis Aquat Organ **95:**65–71. http://dx.doi.org/10.3354/dao02341.
12. **Bakkemo KR, Mikkelsen H, Bordevik M, Torgersen J, Winther-Larsen HC, Vanberg C, Olsen R, Johansen LH, Seppola M.** 2011. Intracellular localisation and innate immune responses following Francisella noatunensis infection of Atlantic cod (Gadus morhua) macrophages. Fish Shellfish Immunol **31:**993–1004. http://dx.doi.org/10.1016/j.fsi.2011.08.020.
13. **Ellis J, Oyston PC, Green M, Titball RW.** 2002. Tularemia. Clin Microbiol Rev **15:**631–646. http://dx.doi.org/10.1128/CMR.15.4.631-646.2002.
14. **Chong A, Wehrly TD, Nair V, Fischer ER, Barker JR, Klose KE, Celli J.** 2008. The early phagosomal stage of Francisella tularensis determines optimal phagosomal escape and Francisella pathogenicity island protein expression. Infect Immun **76:**5488–5499. http://dx.doi.org/10.1128/IAI.00682-08.
15. **Clemens DL, Lee BY, Horwitz MA.** 2009. Francisella tularensis phagosomal escape does not require acidification of the phagosome. Infect Immun **77:**1757–1773. http://dx.doi.org/10.1128/IAI.01485-08.
16. **Santic M, Asare R, Skrobonja I, Jones S, Abu Kwaik Y.** 2008. Acquisition of the vacuolar ATPase proton pump and phagosome acidification are essential for escape of Francisella tularensis into the macrophage cytosol. Infect Immun **76:**2671–2677. http://dx.doi.org/10.1128/IAI.00185-08.
17. **Clemens DL, Lee BY, Horwitz MA.** 2004. Virulent and avirulent strains of Francisella tularensis prevent acidification and maturation of their phagosomes and escape into the cytoplasm in human macrophages. Infect Immun **72:**3204–3217. http://dx.doi.org/10.1128/IAI.72.6.3204-3217.2004.
18. **Golovliov I, Sjöstedt A, Mokrievich A, Pavlov V.** 2003. A method for allelic replacement in Francisella tularensis. FEMS Microbiol Lett **222:**273–280. http://dx.doi.org/10.1016/S0378-1097(03)00313-6.
19. **Lai XH, Golovliov I, Sjöstedt A.** 2001. Francisella tularensis induces cytopathogenicity and apoptosis in murine macrophages via a mechanism that requires intracellular bacterial multiplication. Infect Immun **69:**4691–4694. http://dx.doi.org/10.1128/IAI.69.7.4691-4694.2001.
20. **Santic M, Pavokovic G, Jones S, Asare R, Abu Kwaik Y.** 2010. Regulation of apoptosis and anti-apoptosis signalling by Francisella tularensis. Microbes Infect **12:**126–134. http://dx.doi.org/10.1016/j.micinf.2009.11.003.
21. **Chong A, Wehrly TD, Child R, Hansen B, Hwang S, Virgin HW, Celli J.** 2012. Cytosolic clearance of replication-deficient mutants reveals Francisella tularensis interactions with the autophagic pathway. Autophagy **8:**1342–1356. http://dx.doi.org/10.4161/auto.20808.
22. **Case ED, Chong A, Wehrly TD, Hansen B, Child R, Hwang S, Virgin HW, Celli J.** 2014. The Francisella O-antigen mediates survival in the macrophage cytosol via autophagy avoidance. Cell Microbiol **16:**862–877. http://dx.doi.org/10.1111/cmi.12246.
23. **Cremer TJ, Amer A, Tridandapani S, Butchar JP.** 2009. Francisella tularensis regulates autophagy-related host cell signaling pathways. Autophagy **5:**125–128. http://dx.doi.org/10.4161/auto.5.1.7305.
24. **Steele S, Brunton J, Ziehr B, Taft-Benz S, Moorman N, Kawula T.** 2013. Francisella tularensis harvests nutrients derived via ATG5-independent autophagy to support intracellular growth. PLoS Pathog **9:**e1003562. http://dx.doi.org/10.1371/journal.ppat.1003562.
25. **Checroun C, Wehrly TD, Fischer ER, Hayes SF, Celli J.** 2006. Autophagy-mediated reentry of Francisella tularensis into the endocytic compartment after cytoplasmic replication. Proc Natl Acad Sci U S A **103:**14578–14583. http://dx.doi.org/10.1073/pnas.0601838103.
26. **Jones BD, Faron M, Rasmussen JA, Fletcher JR.** 2014. Uncovering the components of the Francisella tularensis virulence stealth strategy. Front Cell Infect Microbiol **4:**32. http://dx.doi.org/10.3389/fcimb.2014.00032.
27. **Larsson P, Oyston PC, Chain P, Chu MC, Duffield M, Fuxelius HH, Garcia E, Halltorp G, Johansson D, Isherwood KE, Karp PD, Larsson E, Liu Y, Michell S, Prior J, Prior R, Malfatti S, Sjöstedt A, Svensson K, Thompson N, Vergez L, Wagg JK, Wren BW, Lindler LE, Andersson SG, Forsman M, Titball RW.** 2005. The complete genome sequence of

Francisella tularensis, the causative agent of tularemia. Nat Genet **37:**153–159. http://dx.doi.org/10.1038/ng1499.

28. **Nano FE, Zhang N, Cowley SC, Klose KE, Cheung KK, Roberts MJ, Ludu JS, Letendre GW, Meierovics AI, Stephens G, Elkins KL.** 2004. A Francisella tularensis pathogenicity island required for intramacrophage growth. J Bacteriol **186:**6430–6436. http://dx.doi.org/10.1128/JB.186.19.6430-6436.2004.
29. **Nano FE, Schmerk C.** 2007. The Francisella pathogenicity island. Ann N Y Acad Sci **1105:**122–137. http://dx.doi.org/10.1196/annals.1409.000.
30. **Sridhar S, Sharma A, Kongshaug H, Nilsen F, Jonassen I.** 2012. Whole genome sequencing of the fish pathogen Francisella noatunensis subsp. orientalis Toba04 gives novel insights into Francisella evolution and pathogenicity. BMC Genomics **13:**598. http://dx.doi.org/10.1186/1471-2164-13-598.
31. **Long ME, Lindemann SR, Rasmussen JA, Jones BD, Allen LA.** 2013. Disruption of Francisella tularensis Schu S4 iglI, iglJ, and pdpC genes results in attenuation for growth in human macrophages and in vivo virulence in mice and reveals a unique phenotype for pdpC. Infect Immun **81:**850–861. http://dx.doi.org/10.1128/IAI.00822-12.
32. **Santic M, Molmeret M, Barker JR, Klose KE, Dekanic A, Doric M, Abu Kwaik Y.** 2007. A Francisella tularensis pathogenicity island protein essential for bacterial proliferation within the host cell cytosol. Cell Microbiol **9:**2391–2403. http://dx.doi.org/10.1111/j.1462-5822.2007.00968.x.
33. **Santic M, Molmeret M, Klose KE, Jones S, Abu Kwaik Y.** 2005. The Francisella tularensis pathogenicity island protein IglC and its regulator MglA are essential for modulating phagosome biogenesis and subsequent bacterial escape into the cytoplasm. Cell Microbiol **7:**969–979. http://dx.doi.org/10.1111/j.1462-5822.2005.00526.x.
34. **Schmerk CL, Duplantis BN, Howard PL, Nano FE.** 2009. A Francisella novicida pdpA mutant exhibits limited intracellular replication and remains associated with the lysosomal marker LAMP-1. Microbiology **155:**1498–1504. http://dx.doi.org/10.1099/mic.0.025445-0.
35. **Golovliov I, Ericsson M, Sandström G, Tarnvik A, Sjöstedt A.** 1997. Identification of proteins of Francisella tularensis induced during growth in macrophages and cloning of the gene encoding a prominently induced 23-kilodalton protein. Infect Immun **65:**2183–2189.
36. **Lai XH, Golovliov I, Sjöstedt A.** 2004. Expression of IglC is necessary for intracellular growth and induction of apoptosis in murine macrophages by Francisella tularensis. Microb Pathog **37:**225–230. http://dx.doi.org/10.1016/j.micpath.2004.07.002.
37. **Clemens DL, Ge P, Lee BY, Horwitz MA, Zhou ZH.** 2015. Atomic structure of T6SS reveals interlaced array essential to function. Cell **160:**940–951. http://dx.doi.org/10.1016/j.cell.2015.02.005.
38. **Wehrly TD, Chong A, Virtaneva K, Sturdevant DE, Child R, Edwards JA, Brouwer D, Nair V, Fischer ER, Wicke L, Curda AJ, Kupko JJ, III, Martens C, Crane DD, Bosio CM, Porcella SF, Celli J.** 2009. Intracellular biology and virulence determinants of Francisella tularensis revealed by transcriptional profiling inside macrophages. Cell Microbiol **11:**1128–1150. http://dx.doi.org/10.1111/j.1462-5822.2009.01316.x.
39. **Brudal E, Lampe EO, Reubsaet L, Roos N, Hegna IK, Thrane IM, Koppang EO, Winther-Larsen HC.** 2015. Vaccination with outer membrane vesicles from Francisella noatunensis reduces development of francisellosis in a zebrafish model. Fish Shellfish Immunol **42:**50–57. http://dx.doi.org/10.1016/j.fsi.2014.10.025.
40. **Rick Lyons C, Wu TH.** 2007. Animal models of Francisella tularensis infection. Ann N Y Acad Sci **1105:**238–265. http://dx.doi.org/10.1196/annals.1409.003.
41. **Bolger CE, Forestal CA, Italo JK, Benach JL, Furie MB.** 2005. The live vaccine strain of Francisella tularensis replicates in human and murine macrophages but induces only the human cells to secrete proinflammatory cytokines. J Leukoc Biol **77:**893–897. http://dx.doi.org/10.1189/jlb.1104637.
42. **Owen CR, Buker EO, Jellison WL, Lackman DB, Bell JF.** 1964. Comparative studies of Francisella tularensis and Francisella novicida. J Bacteriol **87:**676–683.
43. **Kieffer TL, Cowley S, Nano FE, Elkins KL.** 2003. Francisella novicida LPS has greater immunobiological activity in mice than F. tularensis LPS, and contributes to F. novicida murine pathogenesis. Microbes Infect **5:**397–403. http://dx.doi.org/10.1016/S1286-4579(03)00052-2.
44. **Santic M, Akimana C, Asare R, Kouokam JC, Atay S, Abu Kwaik Y.** 2009. Intracellular fate of Francisella tularensis within arthropod-derived cells. Environ Microbiol **11:**1473–1481. http://dx.doi.org/10.1111/j.1462-2920.2009.01875.x.
45. **Vonkavaara M, Telepnev MV, Ryden P, Sjöstedt A, Stoven S.** 2008. Drosophila melanogaster as a model for elucidating the pathogenicity of Francisella tularensis. Cell Microbiol **10:**1327–1338. http://dx.doi.org/10.1111/j.1462-5822.2008.01129.x.
46. **Brudal E, Ulanova LS, O Lampe E, Rishovd AL, Griffiths G, Winther-Larsen HC.** 2014. Establishment of three Francisella infections in zebrafish embryos at different temperatures. Infect Immun **82:**2180–2194. http://dx.doi.org/10.1128/IAI.00077-14.
47. **Vojtech LN, Sanders GE, Conway C, Ostland V, Hansen JD.** 2009. Host immune response and acute disease in a zebrafish model of Francisella pathogenesis. Infect Immun **77:**914–925. http://dx.doi.org/10.1128/IAI.01201-08.
48. **El-Etr SH, Margolis JJ, Monack D, Robison RA, Cohen M, Moore E, Rasley A.** 2009. Francisella tularensis type A strains cause the rapid encystment of Acanthamoeba castellanii and survive in amoebal cysts for three weeks postinfection. Appl Environ Microbiol **75:**7488–7500. http://dx.doi.org/10.1128/AEM.01829-09.
49. **Lauriano CM, Barker JR, Yoon SS, Nano FE, Arulanandam BP, Hassett DJ, Klose KE.** 2004. MglA regulates transcription of virulence factors necessary for Francisella tularensis intraamoebae and intramacrophage survival. Proc Natl Acad Sci U S A **101:**4246–4249. http://dx.doi.org/10.1073/pnas.0307690101.
50. **Hoffmann C, Harrison CF, Hilbi H.** 2014. The natural alternative: protozoa as cellular models for Legionella infection. Cell Microbiol **16:**15–26. http://dx.doi.org/10.1111/cmi.12235.
51. **Bozzaro S, Eichinger L.** 2011. The professional phagocyte Dictyostelium discoideum as a model host for bacterial pathogens. Curr Drug Targets **12:**942–954. http://dx.doi.org/10.2174/138945011795677782.
52. **Maniak M.** 2002. Conserved features of endocytosis in Dictyostelium. Int Rev Cytol **221:**257–287. http://dx.doi.org/10.1016/S0074-7696(02)21014-1.
53. **Otto GP, Wu MY, Kazgan N, Anderson OR, Kessin RH.** 2003. Macroautophagy is required for multicellular development of the social amoeba Dictyostelium discoideum. J Biol Chem **278:**17636–17645. http://dx.doi.org/10.1074/jbc.M212467200.
54. **Cosson P, Zulianello L, Join-Lambert O, Faurisson F, Gebbie L, Benghezal M, Van Delden C, Curty LK, Kohler T.** 2002. Pseudomonas aeruginosa virulence analyzed in a Dictyostelium discoideum host system. J Bacteriol **184:**3027–3033. http://dx.doi.org/10.1128/JB.184.11.3027-3033.2002.
55. **Hagedorn M, Soldati T.** 2007. Flotillin and RacH modulate the intracellular immunity of Dictyostelium to Mycobacterium marinum infection. Cell Microbiol **9:**2716–2733. http://dx.doi.org/10.1111/j.1462-5822.2007.00993.x.
56. **Solomon JM, Isberg RR.** 2000. Growth of Legionella pneumophila in Dictyostelium discoideum: a novel system for genetic analysis of host-pathogen interactions. Trends Microbiol **8:**478–480. http://dx.doi.org/10.1016/S0966-842X(00)01852-7.
57. **King JS, Gueho A, Hagedorn M, Gopaldass N, Leuba F, Soldati T, Insall RH.** 2013. WASH is required for lysosomal recycling and efficient autophagic and phagocytic digestion. Mol Biol Cell **24:**2714–2726. http://dx.doi.org/10.1091/mbc.E13-02-0092.
58. **Vestvik N, Rønneseth A, Kalgraff CA, Winther-Larsen HC, Wergeland HI, Haugland GT.** 2013. Francisella noatunensis subsp. noatunensis replicates within Atlantic cod (Gadus morhua L.) leucocytes and inhibits respiratory burst activity. Fish Shellfish Immunol **35:**725–733. http://dx.doi.org/10.1016/j.fsi.2013.06.002.
59. **Lindgren H, Honn M, Golovlev I, Kadzhaev K, Conlan W, Sjöstedt A.** 2009. The 58-kilodalton major virulence factor of Francisella tularensis is required for efficient utilization of iron. Infect Immun **77:**4429–4436. http://dx.doi.org/10.1128/IAI.00702-09.
60. **Milton DL, O'Toole R, Horstedt P, Wolf-Watz H.** 1996. Flagellin A is essential for the virulence of Vibrio anguillarum. J Bacteriol **178:**1310–1319.
61. **Simon R, Priefer U, Puhler A.** 1983. A broad host range mobilization system for in vivo genetic-engineering: transposon mutagenesis in Gram-negative bacteria. Biotechnology **1:**784–791. http://dx.doi.org/10.1038/nbt1183-784.
62. **Brudal E, Winther-Larsen HC, Colquhoun DJ, Duodu S.** 2013. Evaluation of reference genes for reverse transcription quantitative PCR analyses of fish-pathogenic Francisella strains exposed to different growth conditions. BMC Res Notes **6:**76. http://dx.doi.org/10.1186/1756-0500-6-76.
63. **Bonquist L, Lindgren H, Golovliov I, Guina T, Sjöstedt A.** 2008. MglA and Igl proteins contribute to the modulation of Francisella tularensis live

vaccine strain-containing phagosomes in murine macrophages. Infect Immun **76:**3502–3510. http://dx.doi.org/10.1128/IAI.00226-08.
64. **Furevik A, Pettersen EF, Colquhoun D, Wergeland HI.** 2011. The intracellular lifestyle of Francisella noatunensis in Atlantic cod (Gadus morhua L.) leucocytes. Fish Shellfish Immunol **30:**488–494. http://dx.doi.org/10.1016/j.fsi.2010.11.019.
65. **Ravanel K, de Chassey B, Cornillon S, Benghezal M, Zulianello L, Gebbie L, Letourneur F, Cosson P.** 2001. Membrane sorting in the endocytic and phagocytic pathway of Dictyostelium discoideum. Eur J Cell Biol **80:**754–764. http://dx.doi.org/10.1078/0171-9335-00215.
66. **Fok AK, Clarke M, Ma L, Allen RD.** 1993. Vacuolar H^+-ATPase of Dictyostelium discoideum. A monoclonal antibody study. J Cell Sci **106:**1103–1113.
67. **Hagedorn M, Neuhaus EM, Soldati T.** 2006. Optimized fixation and immunofluorescence staining methods for Dictyostelium cells. Methods Mol Biol **346:**327–338.
68. **Schneider CA, Rasband WS, Eliceiri KW.** 2012. NIH Image to ImageJ: 25 years of image analysis. Nat Methods **9:**671–675. http://dx.doi.org/10.1038/nmeth.2089.
69. **Kaech A, Ziegler U.** 2014. High-pressure freezing: current state and future prospects. Methods Mol Biol **1117:**151–171. http://dx.doi.org/10.1007/978-1-62703-776-1_8.
70. **Hohenberg H, Mannweiler K, Muller M.** 1994. High-pressure freezing of cell suspensions in cellulose capillary tubes. J Microsc **175:**34–43. http://dx.doi.org/10.1111/j.1365-2818.1994.tb04785.x.
71. **Leonidova A, Pierroz V, Rubbiani R, Lan YJ, Schmitz AG, Kaech A, Sigel RKO, Ferrari S, Gasser G.** 2014. Photo-induced uncaging of a specific Re(I) organometallic complex in living cells. Chem Sci **5:**4044–4056. http://dx.doi.org/10.1039/C3SC53550A.
72. **Duodu S, Larsson P, Sjödin A, Soto E, Forsman M, Colquhoun DJ.** 2012. Real-time PCR assays targeting unique DNA sequences of fish-pathogenic Francisella noatunensis subspecies noatunensis and orientalis. Dis Aquat Organ **101:**225–234. http://dx.doi.org/10.3354/dao02514.
73. **Damer CK, Bayeva M, Kim PS, Ho LK, Eberhardt ES, Socec CI, Lee JS, Bruce EA, Goldman-Yassen AE, Naliboff LC.** 2007. Copine A is required for cytokinesis, contractile vacuole function, and development in Dictyostelium. Eukaryot Cell **6:**430–442. http://dx.doi.org/10.1128/EC.00322-06.
74. **Ashworth JM, Watts DJ.** 1970. Metabolism of the cellular slime mould Dictyostelium discoideum grown in axenic culture. Biochem J **119:**175–182. http://dx.doi.org/10.1042/bj1190175.
75. **Lindgren H.** 2004. Factors affecting the escape of Francisella tularensis from the phagolysosome. J Med Microbiol **53:**953–958. http://dx.doi.org/10.1099/jmm.0.45685-0.
76. **Beyenbach KW, Wieczorek H.** 2006. The V-type H^+ ATPase: molecular structure and function, physiological roles and regulation. J Exp Biol **209:**577–589. http://dx.doi.org/10.1242/jeb.02014.
77. **Lukacs GL, Rotstein OD, Grinstein S.** 1990. Phagosomal acidification is mediated by a vacuolar-type H^+-ATPase in murine macrophages. J Biol Chem **265:**21099–21107.
78. **Clarke M, Maddera L, Engel U, Gerisch G.** 2010. Retrieval of the vacuolar H^+-ATPase from phagosomes revealed by live cell imaging. PLoS One **5:**e8585. http://dx.doi.org/10.1371/journal.pone.0008585.
79. **Gotthardt D, Warnatz HJ, Henschel O, Bruckert F, Schleicher M, Soldati T.** 2002. High-resolution dissection of phagosome maturation reveals distinct membrane trafficking phases. Mol Biol Cell **13:**3508–3520. http://dx.doi.org/10.1091/mbc.E02-04-0206.
80. **Pang KM, Lee E, Knecht DA.** 1998. Use of a fusion protein between GFP and an actin-binding domain to visualize transient filamentous-actin structures. Curr Biol **8:**405–408. http://dx.doi.org/10.1016/S0960-9822(98)70159-9.
81. **Cemma M, Brumell JH.** 2012. Interactions of pathogenic bacteria with autophagy systems. Curr Biol **22:**R540–R545. http://dx.doi.org/10.1016/j.cub.2012.06.001.
82. **Otto GP, Wu MY, Kazgan N, Anderson OR, Kessin RH.** 2004. Dictyostelium macroautophagy mutants vary in the severity of their developmental defects. J Biol Chem **279:**15621–15629. http://dx.doi.org/10.1074/jbc.M311139200.
83. **Froquet R, Cherix N, Burr SE, Frey J, Vilches S, Tomas JM, Cosson P.** 2007. Alternative host model to evaluate Aeromonas virulence. Appl Environ Microbiol **73:**5657–5659. http://dx.doi.org/10.1128/AEM.00908-07.
84. **Hasselbring BM, Patel MK, Schell MA.** 2011. Dictyostelium discoideum as a model system for identification of Burkholderia pseudomallei virulence factors. Infect Immun **79:**2079–2088. http://dx.doi.org/10.1128/IAI.01233-10.
85. **Miyata ST, Kitaoka M, Brooks TM, McAuley SB, Pukatzki S.** 2011. Vibrio cholerae requires the type VI secretion system virulence factor VasX to kill Dictyostelium discoideum. Infect Immun **79:**2941–2949. http://dx.doi.org/10.1128/IAI.01266-10.
86. **Pan YJ, Lin TL, Hsu CR, Wang JT.** 2011. Use of a Dictyostelium model for isolation of genetic loci associated with phagocytosis and virulence in Klebsiella pneumoniae. Infect Immun **79:**997–1006. http://dx.doi.org/10.1128/IAI.00906-10.
87. **MacGurn JA, Hsu PC, Emr SD.** 2012. Ubiquitin and membrane protein turnover: from cradle to grave. Annu Rev Biochem **81:**231–259. http://dx.doi.org/10.1146/annurev-biochem-060210-093619.
88. **Collins CA, De Maziere A, van Dijk S, Carlsson F, Klumperman J, Brown EJ.** 2009. Atg5-independent sequestration of ubiquitinated mycobacteria. PLoS Pathog **5:**e1000430. http://dx.doi.org/10.1371/journal.ppat.1000430.
89. **Rupper A, Cardelli J.** 2001. Regulation of phagocytosis and endophagosomal trafficking pathways in Dictyostelium discoideum. Biochim Biophys Acta **1525:**205–216. http://dx.doi.org/10.1016/S0304-4165(01)00106-4.
90. **Clarke M.** 2010. Recent insights into host-pathogen interactions from Dictyostelium. Cell Microbiol **12:**283–291. http://dx.doi.org/10.1111/j.1462-5822.2009.01413.x.
91. **Fey P, Dodson RJ, Basu S, Chisholm RL.** 2013. One stop shop for everything Dictyostelium: dictyBase and the Dicty Stock Center in 2012. Methods Mol Biol **983:**59–92. http://dx.doi.org/10.1007/978-1-62703-302-2_4.
92. **Reddy TBK, Thomas AD, Stamatis D, Bertsch J, Isbandi M, Jansson J, Mallajosyula J, Pagani I, Lobos EA, Kyrpides NC.** 2015. The Genomes OnLine Database (GOLD) v.5: a metadata management system based on a four level (meta)genome project classification. Nucleic Acids Res **43:**D1099–D1106. http://dx.doi.org/10.1093/nar/gku950.